



# Theoretical constraints on new generations with and without quarks or neutrinos

Alexander Knochel\*, Christof Wetterich

Institut für Theoretische Physik, Ruprecht-Karls-Universität Heidelberg, Germany

## ARTICLE INFO

### Article history:

Received 29 July 2011  
 Received in revised form 11 August 2011  
 Accepted 2 September 2011  
 Available online 6 September 2011  
 Editor: A. Ringwald

## ABSTRACT

We consider large classes of chiral extensions of the Standard Model, including new quark generations that do not involve additional neutrinos as well as lepton generations without quarks. An analysis of renormalization flows of Yukawa and quartic scalar couplings reveals that additional quarks are not compatible with a scenario of grand unification without violating the strong bounds from direct and Higgs searches at colliders. Constraints from direct searches, electroweak precision observables, and Higgs physics, together with the assumption that additional new physics beyond the extended chiral field content should enter significantly above the TeV scale, allows us to make predictions for searches at the LHC.

© 2011 Elsevier B.V. Open access under [CC BY license](http://creativecommons.org/licenses/by/3.0/).

## 1. Introduction

The question whether there are additional chiral fermions beyond the known three generations of quarks and leptons has so far found no conclusive answer. While virtually all models of this type will be tested by the LHC experiments in the near future, the presence of a fourth standard generation of quarks and leptons is still a viable option. However, constraints from flavour physics and the absence of a fourth light neutrino suggest that an additional chiral generation, if present, is not a mere heavy copy of the known three. We therefore also consider alternative anomaly free representations which naturally accommodate the absence of a fourth light neutrino and flavor mixing.

Since the masses of such hypothetical particles must arise via the Higgs mechanism, all such extensions of the Standard Model are tightly constrained due to the tension between collider searches and precision observables on one side, and the renormalization flow of couplings on the other side. In this Letter we argue that all chiral extensions with additional quarks are incompatible with a standard scenario of grand unification. Their existence would require new strong interactions at scales below  $10^7$  GeV. Whenever the scale of such new physics is above a few TeV, the renormalization flow of couplings towards partial fixed points makes such theories highly predictive for the possible values of the masses of new quarks and the Higgs particle, with important consequences for searches at the LHC. We extend our discussion

**Table 1**

The anomaly free hypercharge assignment for an arbitrary number of isospin doublets which allow Yukawa couplings to the Higgs doublet. Representations are given as  $(SU(3), SU(2))_Y$  for left-handed spinors. Electric charges can be read off directly from the hypercharges of the  $SU(2)$  singlets.

Doublets	Singlets	
$(\alpha_1, \mathbf{2})_{A_1}$	$(\bar{\alpha}_1, \mathbf{1})_{-A_1 - \frac{1}{2}}$	$(\bar{\alpha}_1, \mathbf{1})_{-A_1 + \frac{1}{2}}$
$\vdots$	$\vdots$	
$(\alpha_{n_D}, \mathbf{2})_{A_{n_D}}$	$(\bar{\alpha}_{n_D}, \mathbf{1})_{-A_{n_D} - \frac{1}{2}}$	$(\bar{\alpha}_{n_D}, \mathbf{1})_{-A_{n_D} + \frac{1}{2}}$
Anomaly cancellation: $\sum_{i=1}^{n_D}  \alpha_i  A_i = 0$		

to quarkless generations of chiral leptons which may still remain compatible with grand unification.

## 2. Anomaly free representations

In this work we restrict ourselves to isospin doublets which become heavy via the Higgs mechanism. As long as the field content is vectorlike with respect to the  $SU(3)_c$ , there are four anomaly constraints:

$$SU(2)^2 U(1): \sum_{i(SU(2) \text{ doublets})} N_{ci} Y_i = 0, \quad (1)$$

$$SU(3)^2 U(1): \sum_{i(SU(3) \text{ triplets})} Y_i = 0, \quad (2)$$

$$U(1)^3: \sum_{i(\text{all})} N_{ci} Y_i^3 = 0, \quad (3)$$

$$G^2 U(1): \sum_{i(\text{all})} N_{ci} Y_i = 0 \quad (4)$$

\* Corresponding author.

E-mail addresses: [A.K.Knochel@thphys.uni-heidelberg.de](mailto:A.K.Knochel@thphys.uni-heidelberg.de) (A. Knochel), [C.Wetterich@thphys.uni-heidelberg.de](mailto:C.Wetterich@thphys.uni-heidelberg.de) (C. Wetterich).

**Table 2**

Consistent hypercharge assignments for a family of quarks and leptons, for a family of quarks, and for a family consisting of leptons only. Finally, as an example with an odd number of doublets, a family of six quarks is shown which follows the same pattern. Representations are given as  $(SU(3), SU(2))_Y$  for left-handed spinors. Electric charges can be read off directly from the hypercharges of the  $SU(2)$  singlets.

SM4 <sub>Y</sub>	$(\mathbf{3}, \mathbf{2})_A$	$(\bar{\mathbf{3}}, \mathbf{1})_{-A-\frac{1}{2}}$	$(\bar{\mathbf{3}}, \mathbf{1})_{-A+\frac{1}{2}}$
	$(\mathbf{1}, \mathbf{2})_{-3A}$	$(\mathbf{1}, \mathbf{1})_{3A-\frac{1}{2}}$	$(\mathbf{1}, \mathbf{1})_{3A+\frac{1}{2}}$
SM4Q <sub>Y</sub>	$(\mathbf{3}, \mathbf{2})_A$	$(\bar{\mathbf{3}}, \mathbf{1})_{-A-\frac{1}{2}}$	$(\bar{\mathbf{3}}, \mathbf{1})_{-A+\frac{1}{2}}$
	$(\mathbf{3}, \mathbf{2})_{-A}$	$(\bar{\mathbf{3}}, \mathbf{1})_{+A-\frac{1}{2}}$	$(\bar{\mathbf{3}}, \mathbf{1})_{+A+\frac{1}{2}}$
SM4L <sub>Y</sub>	$(\mathbf{1}, \mathbf{2})_A$	$(\mathbf{1}, \mathbf{1})_{-A-\frac{1}{2}}$	$(\mathbf{1}, \mathbf{1})_{-A+\frac{1}{2}}$
	$(\mathbf{1}, \mathbf{2})_B$	$(\mathbf{1}, \mathbf{1})_{-B-\frac{1}{2}}$	$(\mathbf{1}, \mathbf{1})_{-B+\frac{1}{2}}$
	$(\mathbf{1}, \mathbf{2})_C$	$(\mathbf{1}, \mathbf{1})_{-C-\frac{1}{2}}$	$(\mathbf{1}, \mathbf{1})_{-C+\frac{1}{2}}$
	$(\mathbf{1}, \mathbf{2})_D$	$(\mathbf{1}, \mathbf{1})_{-D-\frac{1}{2}}$	$(\mathbf{1}, \mathbf{1})_{-D+\frac{1}{2}}$
	$A + B + C + D = 0$		
SM4Q' <sub>Y</sub>	$(\mathbf{3}, \mathbf{2})_A$	$(\bar{\mathbf{3}}, \mathbf{1})_{-A-\frac{1}{2}}$	$(\bar{\mathbf{3}}, \mathbf{1})_{-A+\frac{1}{2}}$
	$(\mathbf{3}, \mathbf{2})_B$	$(\bar{\mathbf{3}}, \mathbf{1})_{-B-\frac{1}{2}}$	$(\bar{\mathbf{3}}, \mathbf{1})_{-B+\frac{1}{2}}$
	$(\mathbf{3}, \mathbf{2})_C$	$(\bar{\mathbf{3}}, \mathbf{1})_{-C-\frac{1}{2}}$	$(\bar{\mathbf{3}}, \mathbf{1})_{-C+\frac{1}{2}}$
	$A + B + C = 0$		

where sums are over left-handed Weyl spinors. In addition, we would like to allow Yukawa couplings which means for isospin doublets that we introduce complete Dirac fermions in some  $SU(3)_c$  representation which, in terms of left-handed Weyl spinors, satisfy

$$Y(X_L) = -\frac{1}{2} - Y(u_R^c) = \frac{1}{2} - Y(d_R^c). \tag{5}$$

For a number of  $n_D$  independent doublets, this would leave us with up to  $4 + 2n_D$  constraints for  $3n_D$  parameters and thus  $n_D \geq 4$ . The Yukawa conditions are fortunately not independent of the anomaly constraints. They solve the mixed gravitational and  $SU(3)^2U(1)$  constraints for each isospin doublet separately, and reduce the cubic constraint to the  $SU(2)^2U(1)$  constraint,

$$2Y(X_L)^3 + Y(u_R^c)^3 + Y(d_R^c)^3 = -\frac{3}{2}Y(X_L), \tag{6}$$

$$2Y(X_L) + Y(u_R^c) + Y(d_R^c) = 0. \tag{7}$$

This leaves us with a maximum number of  $1 + 2n_D$  constraints for  $3n_D$  parameters, and therefore  $n_D - 1$  free parameters. The general solution is shown in Table 1.

One may furthermore demand an even number of  $SU(2)$  doublets in order to avoid the global  $SU(2)$  anomaly. We do not impose this restriction in view of a possible embedding of the model in higher dimensions for which valid examples with an odd number of four-dimensional chiral doublets are known. Finally, we only consider chiral representations which forbid gauge invariant Dirac masses. An extensive discussion of consistent chiral extensions of the SM can be found in [1]. In the following, we will study the interesting minimal solutions using color triplets (“quarks”) and singlets (“leptons”) only. The solutions to the anomaly and Yukawa constraints for these cases are shown in Table 2. The two simplest nontrivial choices are a family of one quark doublet and one lepton doublet as present in the Standard Model, or two quark doublets and no color singlets. Note that, while the hypercharges of the two isospin doublet quarks in SM4Q<sub>Y</sub> differ only by a sign, the field content is chiral due to the  $SU(3)$  representations, which would not have been the case for a family of two lepton doublets. In SM4<sub>Y</sub>, a fourth Standard Model family is obtained for  $Y = \frac{1}{6}$ . This already exhausts the possibilities if we restrict ourselves to scenarios with one free parameter. The next simplest case with an even number of doublets consists of a family of four lepton

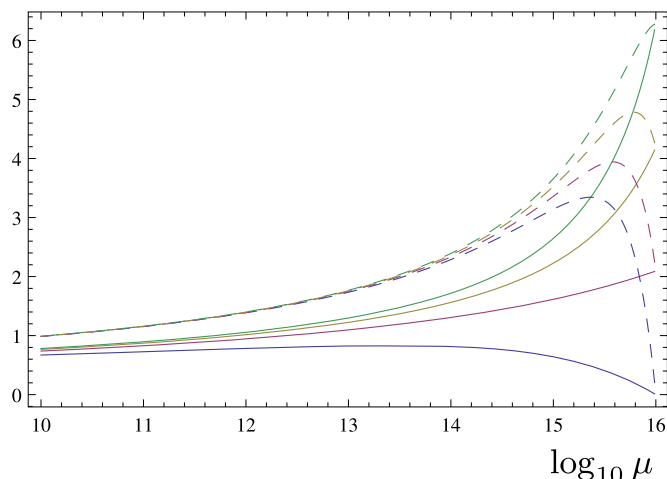


**Fig. 1.** An illustration of the partial fixed point behavior of the quartic Higgs coupling. Shown here is the RG flow in the presence of a Yukawa coupling. We choose initial values for the quartic coupling  $\lambda(10^{16} \text{ GeV}) = 0, \frac{2}{3}\pi, \frac{4}{3}\pi, 2\pi$  and  $h(10^{16} \text{ GeV}) = \frac{\pi}{2}$  (solid) and  $\pi$  (dashed) for the Yukawa coupling. In particular for large Yukawa coupling, the quartic Higgs coupling at low energies becomes almost independent of its value at high scales.

doublets, which can for example be obtained from SM4<sub>Y</sub> by making the quarks color singlets while retaining the multiplicity. This scenario, while having more free parameters, generally allows a higher perturbativity cutoff due to weaker constraints from collider searches, and naively improves the unification of gauge couplings. We also revisit the family of three quark doublets which was found to arise from compactifications of six-dimensional  $SO(12)$  GUTs [2]. The scenario considered there can be obtained from SM4Q' by setting  $A = B = \frac{1}{6}, C = -\frac{1}{3}$ .

The electric charges of baryons and leptons are integer only for specific values of  $A$  for the examples in Table 2, namely  $A = n + \frac{1}{6}$  for SM4, SM4Q and SM4Q'. For SM4Q' not all  $A, B$  and  $C$  can obey this condition, and indeed exotic generations with half-integer charges for baryons and leptons can be obtained from higher dimensional unification [2]. For non-integer charged baryons or leptons the particle with lowest mass must be stable. However, stable baryons with half-integer charge have annihilated very efficiently in early cosmology due to their strong interactions. Their present relic abundance, also in cosmic rays, is too low for detection [3].

The examples SM4Q and SM4Q' involve new quark generations without additional leptons. They are therefore compatible with the LEP bound of three light neutrinos belonging to weak doublets. However, they introduce a large number of color-charged fields and are therefore strongly constrained by Higgs searches. Generations with additional SM-like lepton doublets such as SM4 contain additional sterile neutrinos whose mass is not protected by the gauge symmetries of the Standard Model. This may render such a scenario less attractive.

### 3. An RGE analysis

While the choice of Yukawa couplings and Higgs self coupling seems arbitrary from a low-energy perspective, it turns out that the collective renormalization group running drives the low-energy couplings close to a partial fixed point [4] if one chooses the input parameters at a scale  $\Lambda_c > \Lambda_{EW}$  (Figs. 1 and 2). This can be interpreted as a theoretical prediction from chiral extensions of the Standard Model which do not contain any additional new physics below the scale  $\Lambda_c$ , and no new physics above  $\Lambda_c$  which does not decouple in the low-energy effective theory (e.g. further chiral fermions). If these predictions violate current experimental

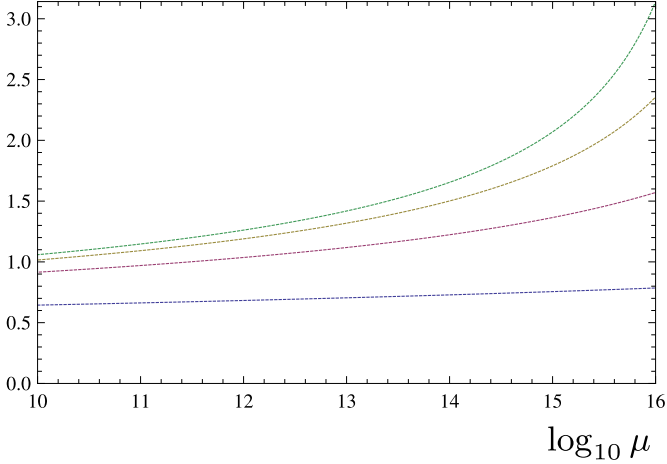


**Fig. 2.** An illustration of the RG flow behavior of the Yukawa coupling. We choose initial values for the Yukawa coupling  $h(10^{16} \text{ GeV}) = \frac{1}{4}\pi, \frac{1}{2}\pi, \frac{3}{4}\pi, \pi$ . For increasing initial Yukawa couplings, the low scale Yukawa coupling saturates.

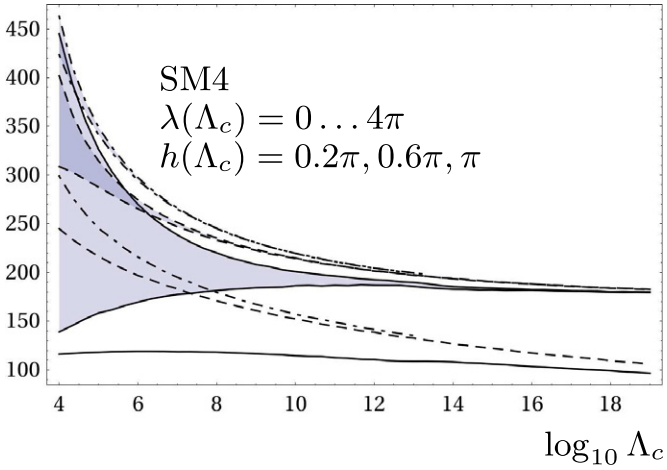


**Fig. 3.** Allowed regions for quark and Higgs boson masses in the SM4. The (degenerate) fourth generation Yukawa couplings are  $h(\Lambda_c) = 0.2\pi$  (solid),  $0.6\pi$  (dashed),  $\pi$  (dot-dashed). For large fourth generation Yukawa couplings, fourth generation masses saturate and  $m_h$  (shaded region) becomes independent of  $\lambda$  as it approaches the partial fixed point. The dot-dashed line ending at  $\Lambda \sim 10^{13} \text{ GeV}$  indicates that the top quark mass could not be accommodated for higher cutoffs.

constraints, we can in return conclude that additional new physics, either weakly interacting such as SUSY or some strongly interacting dynamics, must come in as a remedy.

For  $\Lambda_c$  near some grand unified (GUT) scale, say  $10^{15} \text{ GeV}$  or larger, one finds strong upper bounds for quark masses of additional generations, which is due to the behavior of the Yukawa RG flow (Fig. 2). They conflict with experimental bounds, such that models with additional quark generations require new physics well below the GUT scale. Even much lower  $\Lambda_c$  significantly limits the accessible mass range for the fourth generation fermions and the Higgs boson. This leads to predictive scenarios which are subject to current LHC searches. The situation is illustrated in Figs. 3 and 4, where we show as a function of  $\Lambda_c$  the upper and lower bounds for the Higgs mass for different (but universal) choices of the fourth generation quark Yukawa coupling in the SM4 and SM4Q. The narrow range for the Higgs mass reflects the partial fixed point in  $\lambda/U_4^2$  discussed in [4]. In these plots, it is implied that the top quark mass is fixed at  $m_t \sim 172 \text{ GeV}$ , which leads to upper bounds on  $\Lambda_c$  above which the top mass cannot be produced perturbatively in the presence of the fourth generation Yukawa couplings.

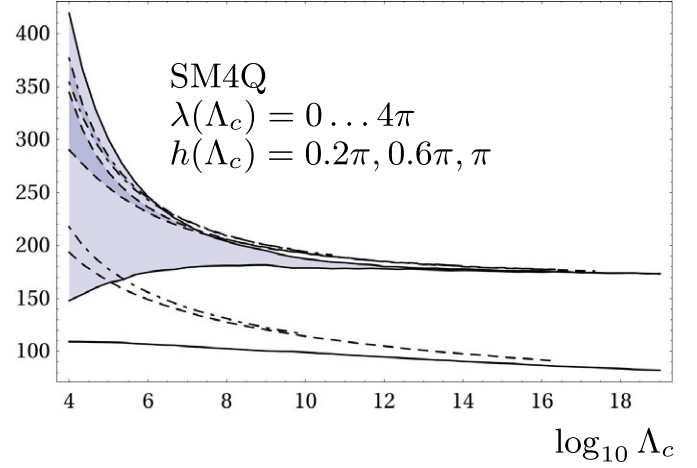


**Fig. 4.** Allowed regions for quark and Higgs boson masses in the SM4Q. The (degenerate) fourth generation Yukawa couplings are  $h(\Lambda_c) = 0.2\pi$  (solid),  $0.6\pi$  (dashed),  $\pi$  (dot-dashed). For large fourth generation Yukawa couplings, fourth generation masses saturate and  $m_h$  (shaded region) becomes independent of  $\lambda$  as it approaches the partial fixed point. The dot-dashed/dashed lines ending at  $\Lambda \sim 10^{10}/10^{16.5} \text{ GeV}$  indicate that the top quark mass could not be accommodated for higher cutoffs.

The one-loop RGEs for the Higgs quartic and Yukawa coupling matrices for arbitrary numbers of quarks and leptons are given by [4]

$$\kappa^{-1}\beta_U = \left( \frac{3}{2}(UU^\dagger - DD^\dagger) + \Sigma - 8g_s^2 - \dots \right) U, \quad (8)$$

$$\kappa^{-1}\beta_D = \left( \frac{3}{2}(DD^\dagger - UU^\dagger) + \Sigma - 8g_s^2 - \dots \right) D, \quad (9)$$

$$\kappa^{-1}\beta_N = \left( \frac{3}{2}(NN^\dagger - LL^\dagger) + \Sigma - \dots \right) N, \quad (10)$$

$$\kappa^{-1}\beta_L = \left( \frac{3}{2}(LL^\dagger - NN^\dagger) + \Sigma - \dots \right) L, \quad (11)$$

$$\kappa^{-1}\beta_\lambda = \left( 12\lambda^2 - 9g_w^2\lambda - \frac{9}{5}g^2\lambda + \frac{3}{4} \left( 3g_w^4 + \frac{6}{5}g_w^2g^2 + \frac{9}{25}g^4 \right) + 4\Sigma\lambda - 4X \right) \quad (12)$$

where  $\kappa^{-1} = 16\pi^2$  and we have defined

$$X = \text{Tr}[3(U^\dagger U)^2 + 3(D^\dagger D)^2 + (L^\dagger L)^2 + (N^\dagger N)^2],$$

$$\Sigma = \text{Tr}[3U^\dagger U + 3D^\dagger D + L^\dagger L + N^\dagger N]. \quad (13)$$

The Yukawa couplings  $U$  for the generalized up-type quarks are rectangular  $L_q \times R_u$  matrices, with  $L_q$  the number of quark doublets, and  $R_u$  the number of up-type singlets. If the up-type quarks have different charges the Yukawa matrix is block diagonal. The same holds for the other Yukawa couplings  $D$  for down-type quarks,  $L$  for charged leptons and  $N$  for neutrino type particles. (Note that neutrino type particles are neutral only for a particular value of the hypercharge in Table 2.) Our convention assumes a tree level Higgs potential of the form  $\mu^2\phi^\dagger\phi + \lambda/2(\phi^\dagger\phi)^2$ . In our numerical analysis, we use the two-loop results from [5,6], neglecting the contributions from electroweak gauge couplings.

We can immediately see that large Yukawa couplings for any field will tend to drive the Yukawa couplings collectively towards smaller values due to the universal positive contribution from  $\Sigma$ , while the running of the quartic coupling receives contributions in both directions from  $X$  and  $\Sigma$ . It is well known that for  $\Lambda_c < M_{Pl}$ , a relatively large range of physical Higgs boson masses can be

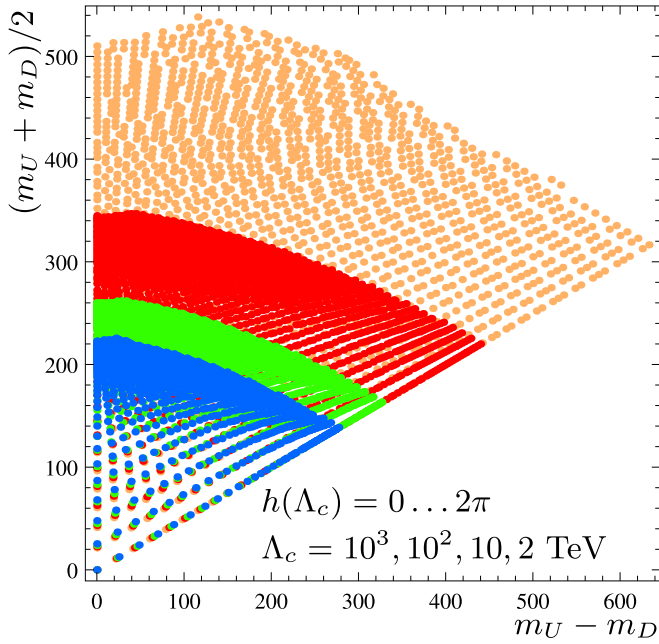


**Fig. 5.** The accessible mass range of fourth generation quarks in the SM4 for high scales  $\Lambda_c = 1000$  (blue), 100 (green), 10 (red), 2 (orange) TeV. The leptons are fixed at 140 GeV and 60 GeV. (For interpretation of the references to color in this figure legend, the reader is referred to the web version of this Letter.)

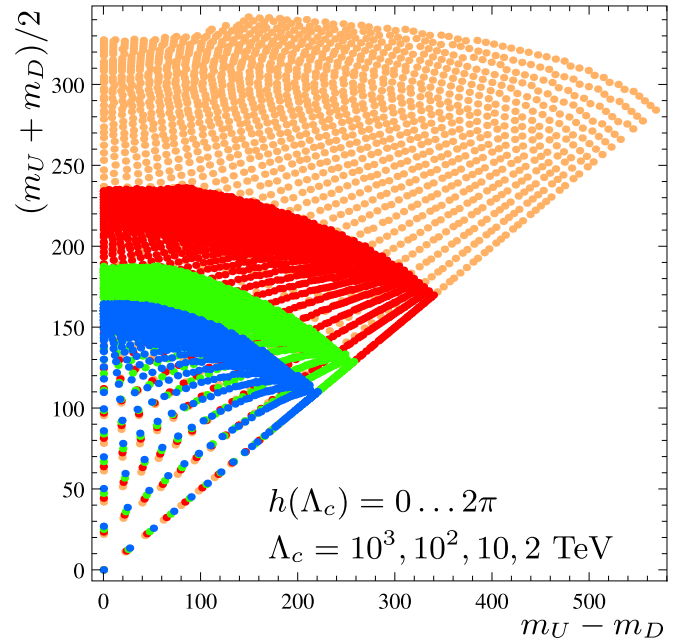


**Fig. 7.** The accessible mass range of fourth generation quarks in the SM4Q for high scales  $\Lambda_c = 1000$  (blue), 100 (green), 10 (red), 2 (orange) TeV. The four quark masses are  $m_{U4} = m_{D5} = m_U$  and  $m_{D4} = m_{U5} = m_D$ . (For interpretation of the references to color in this figure legend, the reader is referred to the web version of this Letter.)

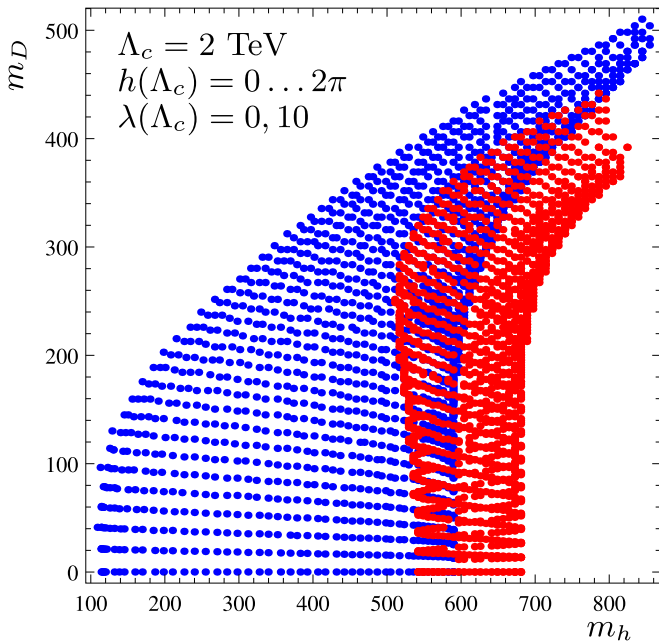


**Fig. 6.** The accessible mass range of the lightest fourth generation quark and the Higgs boson for  $\lambda(\Lambda_c) = 0$  (blue) and  $\lambda(\Lambda_c) = 10$  (red) in the SM4. (For interpretation of the references to color in this figure legend, the reader is referred to the web version of this Letter.)

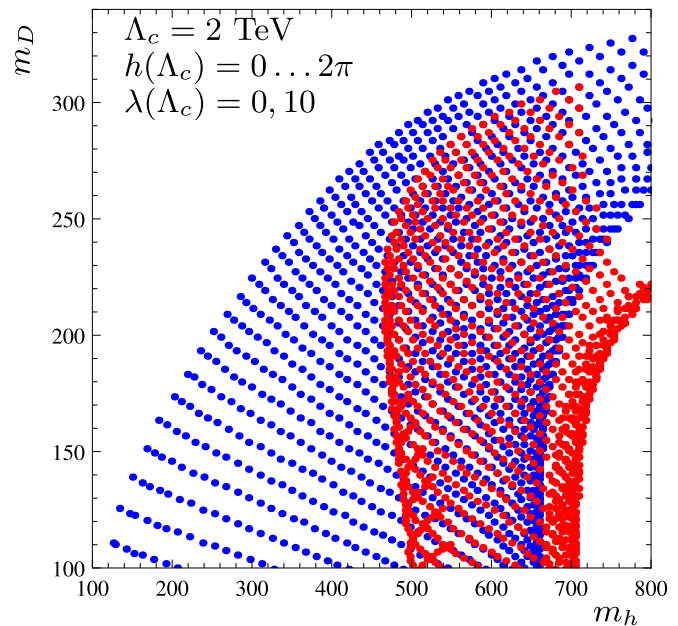


**Fig. 8.** The accessible mass range of the lightest fourth generation quark and the Higgs boson for  $\lambda(\Lambda_c) = 0$  (blue) and  $\lambda(\Lambda_c) = 10$  (red) in the SM4Q. (For interpretation of the references to color in this figure legend, the reader is referred to the web version of this Letter.)

reached in the SM, while additional chiral particle content contributing to  $X$  and  $\Sigma$  will dominate the running of  $\lambda$  and lead to a more precise prediction of  $m_h$  [2]. This behavior is illustrated in Figs. 3 and 4 for the SM4 and SM4Q.

One can now choose a scale  $\Lambda_c$  at which one defines the input parameters (Yukawa and quartic couplings), and evolve them down to the electroweak scale. A scan over the high scale parameters then reveals the accessible mass range of the Higgs and fourth

generation particles as a function of  $\Lambda_c$ . In this analysis, we use the matching condition  $M(\mu_0) = \mu_0$ . The upper bound for the quark mass reflects “triviality” of the running Yukawa couplings. It can be obtained by starting formally with infinite Yukawa couplings  $U_4$  at  $\Lambda_c$  – all smaller initial values will lead to smaller quark masses. For  $\Lambda_c$  of the order of a GUT scale  $10^{15}$  GeV and  $m_t = 172$  GeV, the  $t'$  and  $b'$  quark masses have an upper bound  $m_{t'} = m_{b'} \leq 135$  GeV. If the bound is saturated, the model pre-

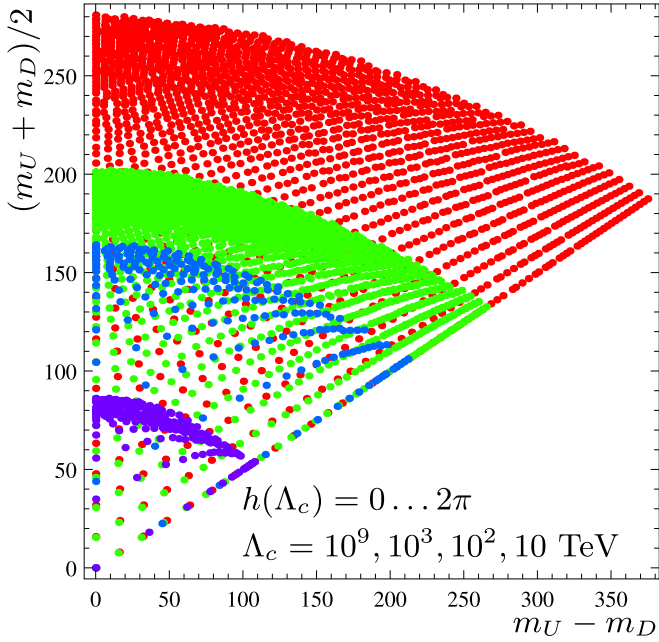


**Fig. 9.** The accessible mass range of fourth generation leptons in the SM4L for high scales  $\Lambda_c = 10^9$  (violet), 1000 (blue), 100 (green), 10 (red) TeV. The masses of the four lepton doublets are chosen to be  $m_{N4\dots N6} = m_{L7} = m_U$  and  $m_{L4\dots L6} = m_{N7} = m_D$ . (For interpretation of the references to color in this figure legend, the reader is referred to the web version of this Letter.)

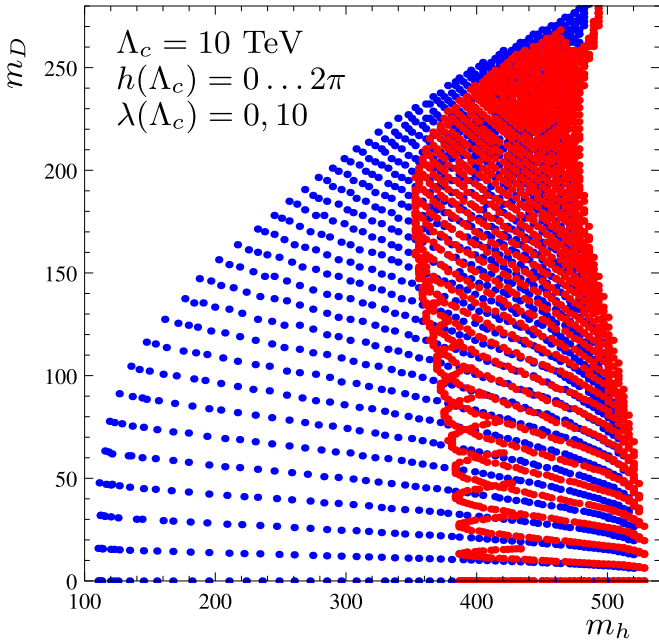


**Fig. 10.** The accessible mass range of the lightest fourth generation quark and the Higgs boson for  $\lambda(\Lambda_c) = 0$  (blue) and  $\lambda(\Lambda_c) = 10$  (red) in the SM4L. (For interpretation of the references to color in this figure legend, the reader is referred to the web version of this Letter.)

dicts a Higgs mass  $m_H \sim 192$  GeV. These exotic quark masses are far outside present experimental bounds. Bounds for SM4Q ( $m_{t_i} = m_{b_i} \leq 100$  GeV) or SM4Q' ( $m_{t_i} = m_{b_i} \leq 82$  GeV) are even stronger. We conclude that additional quark generations are not compatible with grand unification.

In this context we denote by “grand unification” a class of models with gauge group  $SU(3) \times SU(2) \times U(1)$  (or slight extensions

as additional  $U(1)$  factors) that are valid up to a high scale (say  $\Lambda_c > 10^{12}$  GeV) without invoking new strong interactions involving so far undetected particles at intermediate scales. The content of chiral fermions is left arbitrary. (Additional vectorlike fermions or an extended Higgs sector will not modify substantially the upper bound for  $m_{q_4}$ .) The only way to escape the upper bound for  $m_{q_4}$  in this setting would be a replacement of the triviality of Yukawa couplings by a fixed point behavior for large values of the Yukawa couplings [4,7–9]. So far, lattice [10,11] or functional renormalization group studies [4,7–9] have not found such a fixed point in the “grand unification setting”. (A possible exception could be models with strong four-fermion interactions [8].)

Abandoning the GUT scenario new strong interactions would have to occur at rather low scales  $\Lambda_c$  in a range below  $10^7$  GeV. In the following we investigate this “strong interaction scenario”. We show that for  $\Lambda_c > 10$  TeV the heavy particle masses are already strongly constrained. The results for the fourth generation quark masses in the SM4 are shown in Fig. 5. We emphasize the strong clustering of points near the upper bound. The corresponding results for the lepton-less scenario SM4Q and the quark-less scenario SM4L are shown in Figs. 7 and 9. The dependence on the value of the quartic coupling at the high scale is strongly reduced for large fourth generation masses. This is illustrated in Figs. 6, 8 and 10.

We have considered the quark-less scenario SM4L at a very high cutoff scale. The motivation for this is that the extension of the SM by color-neutral fields can improve the precision of gauge unification. At one-loop, for SM-like charge assignments  $3A = 3B = 3C = -D$ , we find  $\frac{\alpha_Y^{-1} - \alpha_L^{-1}}{\alpha_Y^{-1} - \alpha_S^{-1}} = 1 - \frac{155}{576D^2 + 357}$ , which is roughly in agreement with the measured value for  $|D| \lesssim \frac{1}{2}$ . At two-loop, the Yukawa couplings enter and have a significant impact on the precision of unification. In particular in scenarios with new color-charged fields where the Yukawa couplings blow up far below the unification scale, it is therefore not sensible to consider the perturbative running of gauge couplings. The scale of unification without additional color-charged fields (at one-loop) is around  $10^{12\dots 13}$  GeV.

Furthermore, the masses in this scenario are least constrained by direct searches. We find that the upper bounds on the exotic lepton masses (which cannot all be made neutral) are very close to or below the exclusion bounds from collider searches.

#### 4. Electroweak precision tests

One of the most stringent experimental bounds on new chiral particle content comes from electroweak precision observables, and in particular the oblique corrections to gauge boson self-energies. A very convenient parametrization of these corrections is given by the Peskin–Takeuchi STU parameters [12]. We use the approximate expressions for the contributions of heavy isospin doublets to  $S$  and  $T$ , [12,13],

$$\Delta T = \frac{N_c}{16\pi s_w^2 m_W^2} \left( m_U^2 + m_D^2 - \frac{m_U^2 m_D^2}{m_U^2 - m_D^2} \log \frac{m_U^2}{m_D^2} \right),$$

$$\Delta S = \frac{N_c}{6\pi} \left( 1 - 2Y \log \frac{m_U^2}{m_D^2} \right) \quad (14)$$

which have been considered in a similar analysis by [14] and agree with the full electroweak calculation sufficiently for our purposes.  $\Delta T$ , which measures the violation of custodial symmetry by the splitting of isospin doublets, is positive semidefinite, while  $\Delta S$  can be made small or negative by the splitting. This works best if  $|Y|$  of the doublets is large. The contributions to  $S$  and  $T$  from physics beyond the SM are tightly constrained by experiments [15,16]. In

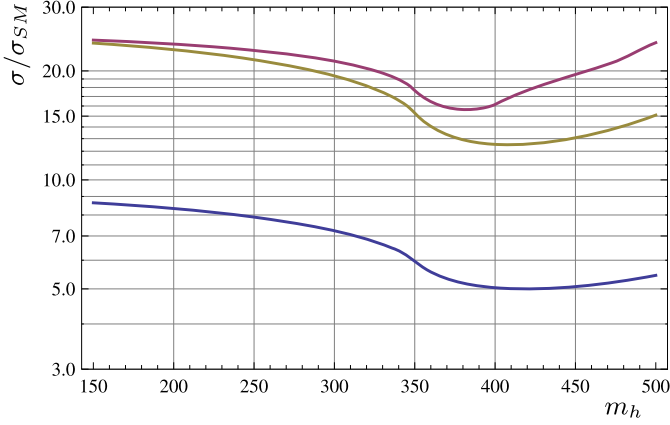


**Fig. 11.** The strength of the effective  $ggH$  coupling relative to the SM expressed in terms of production cross sections. The scenarios shown are (from weakest to strongest) the SM4 ( $m_U = 310$  GeV,  $m_D = 260$  GeV), the SM4Q ( $m_U = 310$  GeV,  $m_D = 280$  GeV) and again the SM4Q ( $m_U = 240$  GeV,  $m_D = 200$  GeV).

the  $\Lambda \geq 10$  TeV scenarios with heavy fourth generation Quarks, we generically find Higgs masses  $m_H > 200 \dots 300$  GeV. Such a heavy Higgs boson contributes to  $S$  and  $T$ , shifting the preferred range for  $\Delta S$  and  $\Delta T$  to smaller/larger values respectively. The impact of the Higgs spectrum and new chiral particle content on oblique corrections has been studied thoroughly for example in [17]. In order to combine our results from the RGE analysis with the electroweak constraints in a meaningful way, we check for each point of the scan whether  $\Delta S$  and  $\Delta T$  lie within the 68% CL or the 95% CL ellipse given by [16,15]. First we consider the SM4 with standard hypercharge assignments  $Y(Q) = \frac{1}{6}$ . The result is shown in Figs. 12, 13. The lepton and neutrino masses which are not shown are fixed at 140 GeV and 60 GeV respectively. The SM4Q does not pass electroweak precision tests for the SM-like hypercharge assignment  $Y(Q) = \frac{1}{6}$  due to the large field content. However, for  $Y(Q) = 1$ , the cancellation of  $\Delta S$  is more effective and a range of masses becomes allowed by precision tests (Figs. 14, 15). The SM4L for  $Y(L_{1\dots 3}) = \frac{1}{6}$  and  $Y(L_4) = -\frac{1}{2}$  yields results similar to the SM4 case due to the identical field content and hypercharges (Figs. 16, 17). As an interesting variation, we consider the case  $Y(L_{1\dots 3}) = -\frac{1}{2}$  and  $Y(L_4) = \frac{3}{2}$  where three doublets are SM-like with neutral neutrinos, while the fourth doublet has electrical charges 1 and 2. In this case, having light exotic neutrinos gives small corrections to  $S$  and is advantageous in order to evade direct searches. Consequently, a relatively large range of parameter space is allowed by electroweak precision tests (Figs. 18, 19). We can raise the scale to  $\Lambda_c = 10^{12}$  GeV and still find a range of viable parameter points for the SM-like charge assignment (Figs. 20, 21).

## 5. Higgs production

The contributions of chiral matter to the effective  $Hgg$ , and  $H\gamma\gamma$  operators do not decouple for  $m \gg m_H$ , which makes Higgs production and decay an important probe of models with chiral particle content beyond the SM. In particular at the LHC, the production of Higgs bosons is dominated by  $gg \rightarrow H$  for the entire accessible mass range, which results in a production rate roughly proportional to  $N_f^2$  where  $N_f$  is the number of heavy  $SU(3)$  triplets. The coupling to photons receives contributions from  $W$  boson loops, which interfere destructively with heavy charged fermionic matter, which generically leads to a reduction of  $\Gamma(H \rightarrow \gamma\gamma)$  except in extreme cases with many or multiply charged particles. The partial widths for  $H \rightarrow \gamma\gamma$  and  $H \rightarrow gg$  can be written as [18,14]

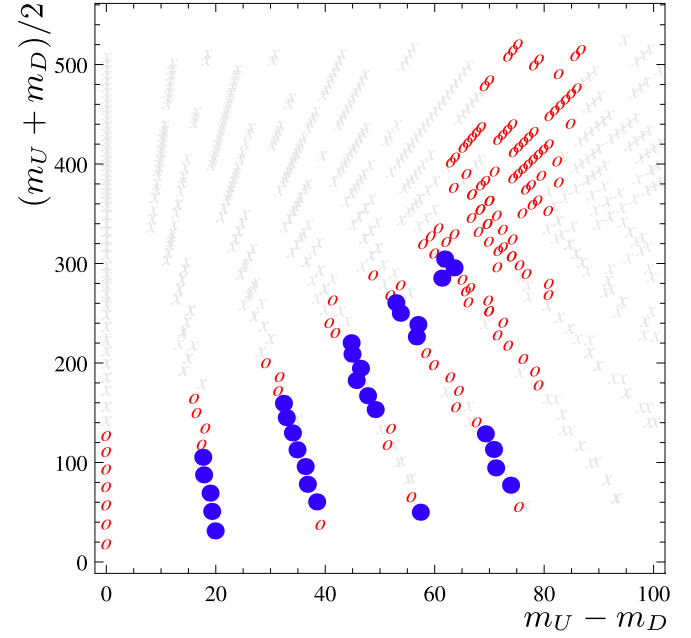


**Fig. 12.** The points in the SM4 ( $Y = \frac{1}{6}$ ,  $\Lambda_c = 2$  TeV,  $\lambda(\Lambda_c) = 0, 10$ ) which are not excluded by electroweak precision tests at 68% CL/95% CL are shown as blue dots/red circles. (For interpretation of the references to color in this figure legend, the reader is referred to the web version of this Letter.)

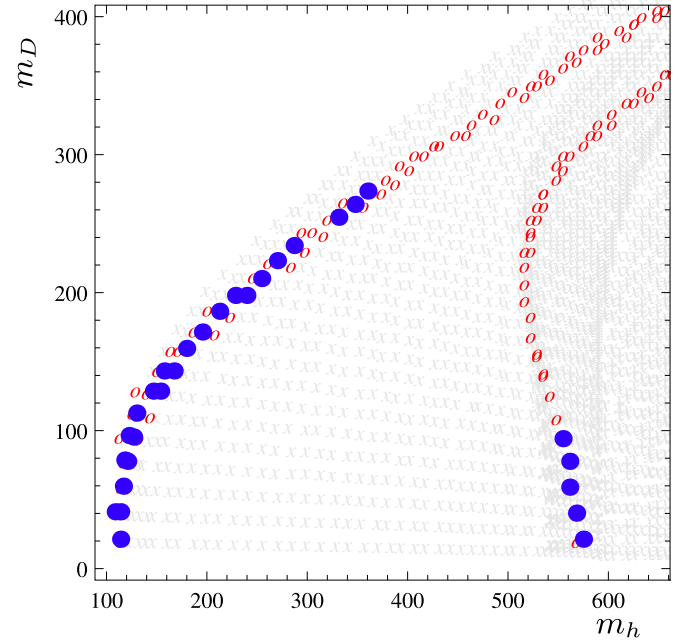


**Fig. 13.** The points in the SM4 ( $Y = \frac{1}{6}$ ,  $\Lambda_c = 2$  TeV,  $\lambda(\Lambda_c) = 0, 10$ ) which are not excluded by electroweak precision tests at 68% CL/95% CL are shown as blue dots/red circles. (For interpretation of the references to color in this figure legend, the reader is referred to the web version of this Letter.)

$$\Gamma_{H \rightarrow \gamma\gamma} = \frac{G_\mu \alpha^2 m_H^3}{128 \sqrt{2} \pi^3} \left| \sum_f N_c Q_f^2 A_f(\tau_f) + A_W(\tau_W) \right|^2,$$

$$\Gamma_{H \rightarrow gg} = \frac{G_\mu \alpha_s^2 m_H^3}{36 \sqrt{2} \pi^3} \left| \frac{3}{4} \sum_f A_f(\tau_f) \right|^2, \quad (15)$$

where the form factors  $A_f$  and  $A_W$  for  $s = \frac{1}{2}$  and  $s = 1$  fields are given by

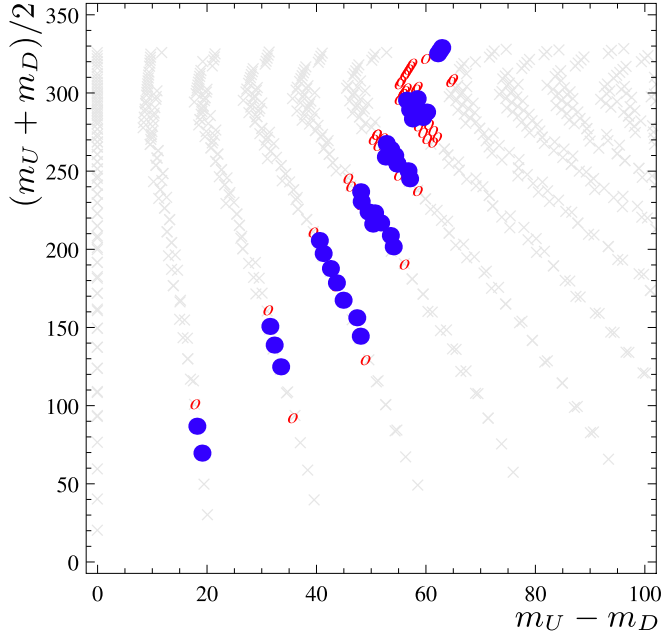


**Fig. 14.** The points in the SM4Q ( $Y = 1$ ,  $\Lambda_c = 2$  TeV,  $\lambda(\Lambda_c) = 0, 10$ ) which are not excluded by electroweak precision tests at 68% CL/95% CL are shown as blue dots/red circles. (For interpretation of the references to color in this figure legend, the reader is referred to the web version of this Letter.)

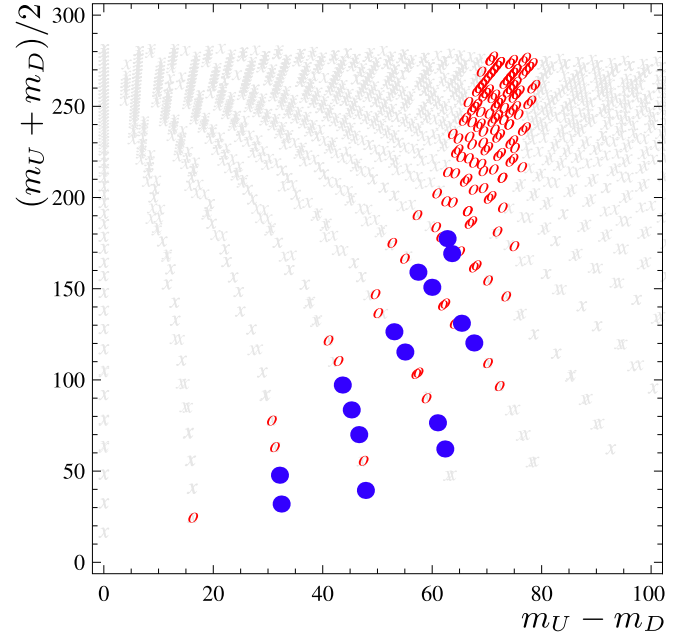


**Fig. 16.** The points in the SM4L ( $Y = \frac{1}{6}$ ,  $\Lambda_c = 10$  TeV,  $\lambda(\Lambda_c) = 0, 10$ ) which are not excluded by electroweak precision tests at 68% CL/95% CL are shown as blue dots/red circles. (For interpretation of the references to color in this figure legend, the reader is referred to the web version of this Letter.)

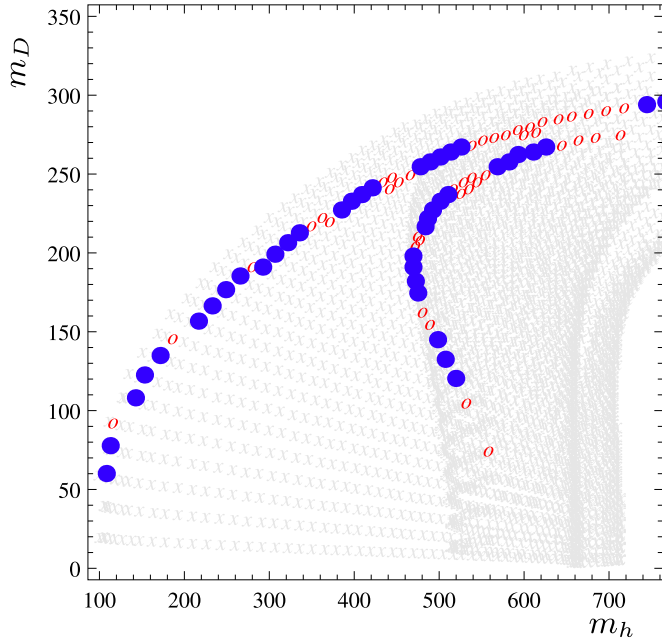


**Fig. 15.** The points in the SM4Q ( $Y = 1$ ,  $\Lambda_c = 2$  TeV,  $\lambda(\Lambda_c) = 0, 10$ ) which are not excluded by electroweak precision tests at 68% CL/95% CL are shown as blue dots/red circles. (For interpretation of the references to color in this figure legend, the reader is referred to the web version of this Letter.)

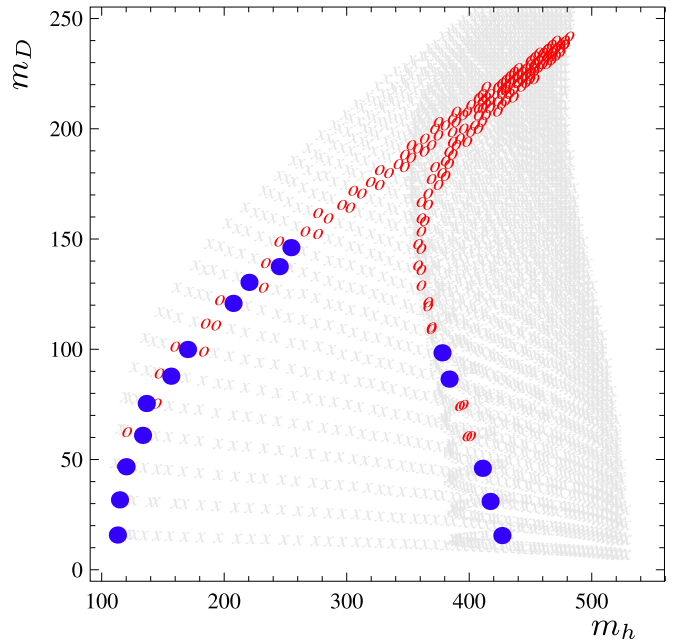


**Fig. 17.** The points in the SM4L ( $Y = \frac{1}{6}$ ,  $\Lambda_c = 10$  TeV,  $\lambda(\Lambda_c) = 0, 10$ ) which are not excluded by electroweak precision tests at 68% CL/95% CL are shown as blue dots/red circles. (For interpretation of the references to color in this figure legend, the reader is referred to the web version of this Letter.)

$$A_f(\tau) = 2[\tau + (\tau - 1)f(\tau)]\tau^{-2},$$

$$A_W(\tau) = -[2\tau^2 + 3\tau + 3(2\tau - 1)f(\tau)]\tau^{-2} \quad (16)$$

with  $\tau_i = m_H^2/4m_i^2$  ( $i = f, W$ ) and

$$f(\tau) = \begin{cases} \arcsin^2 \sqrt{\tau}, & \tau \leq 1, \\ -\frac{1}{4}[\ln \frac{1+\sqrt{1-\tau^{-1}}}{1-\sqrt{1-\tau^{-1}}} - i\pi]^2, & \tau > 1. \end{cases} \quad (17)$$

The partial widths are proportional to the strength of the effective  $ggH$  operator in Higgs production since we assume an onshell Higgs boson in both cases, and kinematics cancel for identical Higgs masses. We thus use the same form factors to estimate the enhancement of  $gg \rightarrow H$  production rates relative to the SM. The result for three scenarios is shown in Fig. 11. We observe that the enhancement is considerably weaker than the naive estimate  $\sigma \propto N_f^2$  which assumes  $m_{qf} \rightarrow \infty$ .

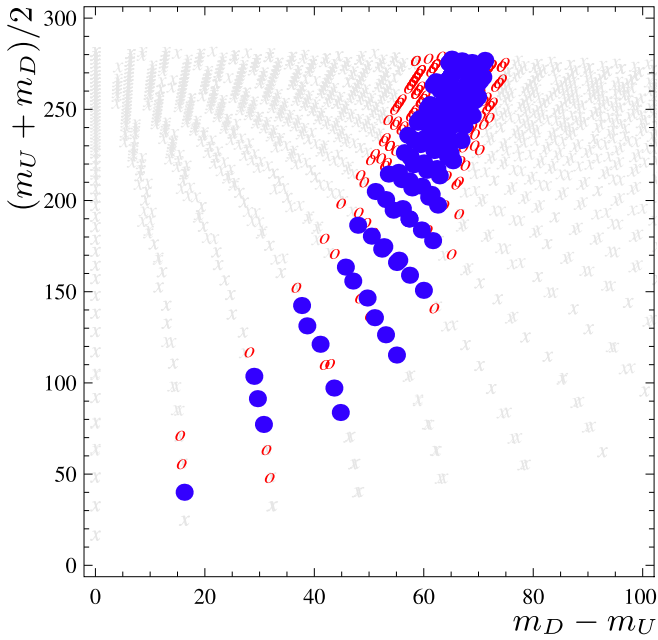


**Fig. 18.** The points in the SM4L ( $Y = -\frac{1}{2}$ ,  $\Lambda_c = 10$  TeV,  $\lambda(\Lambda_c) = 0, 10$ ) which are not excluded by electroweak precision tests at 68% CL/95% CL are shown as blue dots/red circles. (For interpretation of the references to color in this figure legend, the reader is referred to the web version of this Letter.)

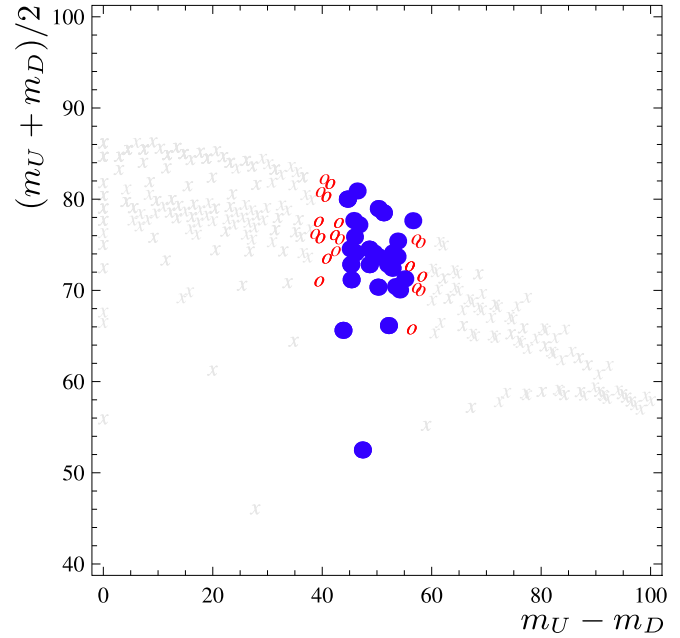


**Fig. 20.** The points in the SM4L ( $Y = \frac{1}{6}$ ,  $\Lambda_c = 10^{12}$  GeV,  $\lambda(\Lambda_c) = 0, 10$ ) which are not excluded by electroweak precision tests at 68% CL/95% CL are shown as blue dots/red circles. (For interpretation of the references to color in this figure legend, the reader is referred to the web version of this Letter.)

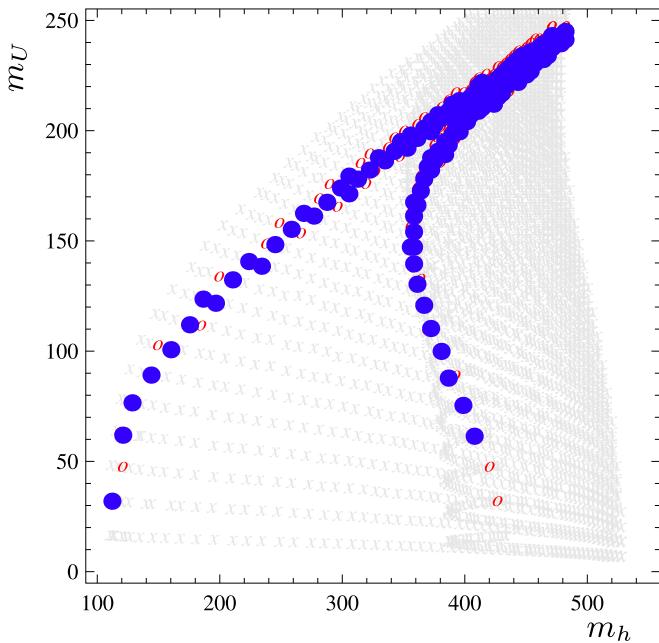


**Fig. 19.** The points in the SM4L ( $Y = -\frac{1}{2}$ ,  $\Lambda_c = 10$  TeV,  $\lambda(\Lambda_c) = 0, 10$ ) which are not excluded by electroweak precision tests at 68% CL/95% CL are shown as blue dots/red circles (For interpretation of the references to color in this figure legend, the reader is referred to the web version of this Letter.)

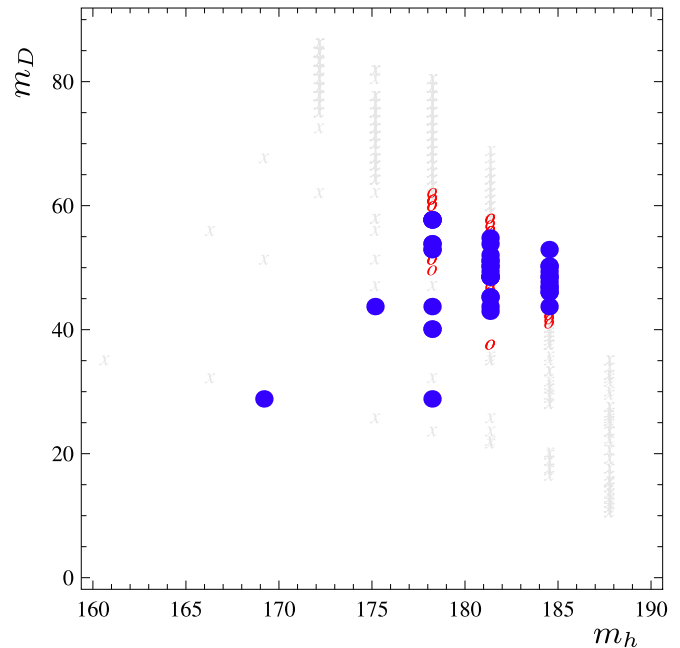


**Fig. 21.** The points in the SM4L ( $Y = \frac{1}{6}$ ,  $\Lambda_c = 10^{12}$  GeV,  $\lambda(\Lambda_c) = 0, 10$ ) which are not excluded by electroweak precision tests at 68% CL/95% CL are shown as blue dots/red circles. (For interpretation of the references to color in this figure legend, the reader is referred to the web version of this Letter.)

**6. Conclusions**

Nevertheless, for most values of  $m_h$ , the scenarios with more than one new quark doublet are already excluded by Higgs searches at the LHC unless one does invoke additional invisible decay modes for the Higgs which compete with  $h \rightarrow WW, ZZ$ . For the scenario without additional quarks, there is no such constraint.

We have investigated the simplest classes of anomaly free chiral extensions of the Standard Model, namely a generalization of the usual fourth generation scenario, a family of two and three quark doublets, and a family of exotic leptons. From our renormalization group analysis we conclude that the experimental lower bounds on fourth generation quark masses have already forced such models into a regime where additional new physics beyond



the extra generation is necessary below a scale of  $10^2 \dots 10^3$  TeV. A fourth generation containing quarks is not compatible with a scenario of grand unification, unless one invokes a fixed point for strong Yukawa couplings for which there is no evidence so far. The neutrinoless fourth generation of quarks faces particularly strong constraints, since the enhanced chiral particle content (six new doublets rather than four as in the SM4 case) both contributes very significantly to Higgs production cross sections, and results in a lower mass window. The fourth generation of leptons is less constrained by direct searches, which allows us to raise the cutoff close to the putative unification scale  $\Lambda \sim 10^{12}$  GeV. As the experimental bounds for exotic fermion masses rise, the RGE evolution of the quartic scalar coupling is dominated by the contributions from fourth generation Yukawa couplings, and the expected Higgs boson mass is typically above  $200 \dots 300$  GeV. This has an important effect on electroweak precision tests. In order to illustrate this, we have analyzed the contributions to oblique corrections in several selected scenarios which remain perturbative above  $\Lambda_c \geq 2 \dots 10$  TeV. We find that conventional fourth generation models and a color-neutral fourth generation pass electroweak precision tests for a range of masses, while scenarios with more than one additional quark doublet pass electroweak precision tests only for suitable hypercharge assignments. In view of Fig. 11, LHC seems to have the potential to definitely close the window for new quark generations.

## Acknowledgements

We thank A. Hebecker, K. Matchev, T. Plehn and C. Speckner for useful discussions. AK would like to thank the University of Florida, Gainesville for hospitality while parts of this work were finished.

## References

- [1] R. Foot, H. Lew, R.R. Volkas, G.C. Joshi, Phys. Rev. D 39 (1989) 3411.
- [2] C. Wetterich, Phys. Lett. B 167 (1986) 325.
- [3] G. Ingelmann, C. Wetterich, Phys. Lett. B 174 (1986) 109.
- [4] C. Wetterich, Phys. Lett. B 104 (1981) 269.
- [5] M.-x. Luo, Y. Xiao, Phys. Rev. Lett. 90 (2003) 011601, hep-ph/0207271.
- [6] M.-x. Luo, H.-w. Wang, Y. Xiao, Phys. Rev. D 67 (2003) 065019, hep-ph/0211440.
- [7] S. Bornholdt, C. Wetterich, Phys. Lett. B 282 (1992) 399.
- [8] H. Gies, J. Jaeckel, C. Wetterich, Phys. Rev. D 69 (2004) 105008.
- [9] H. Gies, S. Rechenberger, M. Scherer, Eur. Phys. J. C 66 (2010) 403.
- [10] J. Kuti, L. Lin, Y. Shen, Phys. Rev. Lett. 61 (1988) 678.
- [11] P. Gerhald, K. Jansen, JHEP 0710 (2007) 001.
- [12] M.E. Peskin, T. Takeuchi, Phys. Rev. D 46 (1992) 381.
- [13] B.A. Kniehl, H.-G. Kohrs, Phys. Rev. D 48 (1993) 225.
- [14] G.D. Kribs, T. Plehn, M. Spannowsky, T.M. Tait, Phys. Rev. D 76 (2007) 075016, arXiv:0706.3718.
- [15] K. Nakamura, et al., Particle Data Group, J. Phys. G 37 (2010) 075021.
- [16] M. Baak, et al., Gitter Collaboration, PoS EPS-HEP2009 (2009) 254.
- [17] H.-J. He, N. Polonsky, S.-f. Su, Phys. Rev. D 64 (2001) 053004, hep-ph/0102144.
- [18] J.R. Ellis, M.K. Gaillard, D.V. Nanopoulos, Nucl. Phys. B 106 (1976) 292.